Reg Environ Change
DOI 10.1007/s10113-013-0495-6

ORIGINAL ARTICLE

Evidence for a warm and humid Mid-Holocene episode in the Aegean and northern Levantine Seas (Greece, NE Mediterranean)

M. V. Triantaphyllou · A. Gogou · I. Bouloubassi · M. Dimiza · K. Kouli · G. Rousakis · U. Kotthoff · K.-C. Emeis · M. Papanikolaou · M. Athanasiou · C. Parinos · C. Ioakim · V. Lykousis

Received: 21 October 2012 / Accepted: 9 June 2013

Abstract Marine and terrestrial biological and biogeochemical proxies in three sediment cores from North and SE Aegean and northern Levantine Seas record continuous warm and humid conditions between 5.5 and 4.0 ka BP related to the establishment of relatively stratified conditions in the upper water column. These conditions may have resulted from the concordant albeit weak Mid-Holocene South Asian monsoon forcing, combined with lighter Etesian winds. During this interval, sea surface temperatures fluctuate in the Aegean Sea, although exhibiting a strong positive shift at ~4.8 ka BP. The warm and humid climatic conditions triggered upper water column stratification and enhancement of the deep chlorophyll maximum (DCM), leading to dysoxic conditions and the deposition of a sapropel-like layer, but only in the SE Aegean site. In contrast to the shallow water SE Aegean, the deeper North Aegean and the northern Levantine sites, although experiencing stratification in the upper parts of the water column, did not achieve bottom-water dysoxia. Thus, a top–bottom mechanism of stratification–DCM development accompanied by fast transport and burial of organic matter is a likely explanation for the preservation of productivity signal in the shallow sites of the SE Aegean and establishment of sapropelic conditions during the warm and humid Mid-Holocene. The termination of the Mid-Holocene warm and humid phase coincides with the "4.2 ka" climate event. Our data exhibit an N–S time transgressive aridification gradient around the Aegean Sea, most probably associated with the reorganization of the general atmospheric circulation during the Mid-Holocene.

Keywords Mid-Holocene · NE Mediterranean · Warm · Humid · Climate · Multiproxy

M. V. Triantaphyllou (✉) · M. Dimiza · K. Kouli · M. Papanikolaou · M. Athanasiou
Faculty of Geology and Geoenvironment, National and Kapodistrian University of Athens, Panepistimiopolis, 15784 Athens, Greece
e-mail: mtriant@geol.uoa.gr

A. Gogou · G. Rousakis · C. Parinos · V. Lykousis
Institute of Oceanography, Hellenic Centre for Marine Research, 19013 Anavyssos, Greece

I. Bouloubassi
Laboratoire d'Océanographie et du Climat, Expérimentation et Approche Numérique, Université Pierre et Marie Curie, Paris Cedex 05, France

U. Kotthoff
Geologisch-Paläontologisches Institut und Museum, Universität Hamburg, Bundesstr. 55, 20146 Hamburg, Germany

K.-C. Emeis
Institut für Biogeochemie und Meereschemie, Universität Hamburg, Bundesstr. 55, 20146 Hamburg, Germany

C. Ioakim
Institute of Geology and Mineral Exploration, Olympic Village, 13677 Acharnae-Attiki, Greece

Introduction

The mid-latitude, semi-enclosed Mediterranean Sea is a small-scale ocean with high environmental variability and steep physicochemical gradients (Bethoux et al. 1999). Climatically, it is influenced by both tropical and mid-latitude climate processes (Lionello et al. 2006) and its physical, chemical and biological environments have reacted sensitively to climate variability in the past (e.g. Cacho et al. 2002; Rohling et al. 2002a; Tzedakis et al. 2004; Margari et al. 2009) and in the present (e.g. Theocharis et al. 1999; Zervakis et al. 2000). The climatic

Published online: 29 June 2013

changes imprinted in the sedimentary archive of the Mediterranean Sea are closely linked to both the global atmospheric teleconnection patterns and shifts in the Intertropical Convergence Zone (ITCZ) over Africa (Lutterbacher and Xoplaki 2003; Rohling et al. 2009).

Dramatically different oceanographic and environmental conditions in the past have resulted in the (quasi) periodic occurrence of organic-rich layers known as sapropels in the eastern Mediterranean (Hilgen et al. 2003; Emeis et al. 2003). Sapropels developed in concert with maximum insolation gradient between the Tropic of Cancer and the Equator (e.g. Rossignol-Strick et al. 1982), when the related precession-driven intensification of the western African monsoon promoted an increased freshwater discharge from the north African rivers, possibly supplemented by enhanced freshwater inputs from the southern European and southwest Asian margins (e.g. Rohling et al. 2002a; Kotthoff et al. 2008a). Subsequently, freshwater stratification and organic carbon accumulation took place due to both productivity and hypoxia, during warm and wet climatic conditions (e.g. de Lange and Ten Haven 1983; Emeis et al. 2003; Moodley et al. 2005; Möbius et al. 2010). The most recent sapropel S1 was deposited in between 10.8 and 6.1 ka BP (de Lange et al. 2008) during reduced deep-water formation and bottom ventilation (e.g. Meier et al. 2004; Schmiedl et al. 2010; Katsouras et al. 2010).

In the NE Mediterranean, the Aegean sub-basin has a crucial role in the Mediterranean thermohaline circulation (e.g. Theocharis et al. 1999). The Aegean Sea represents a natural laboratory recording high latitude variability (Rohling et al. 2002b). In winter, the Aegean Sea is under the direct influence of northerly winds and precipitation regimes, and sedimentation patterns reflect variations in high-latitude forced climate, whereas during summer, the wind field is dominated by the presence of the Etesian wind, blowing mainly from the north (e.g. Poulos 2009). In the northern Aegean antagonistic influences of freshwater influx from the Black Sea (Zervakis et al. 2000) and rivers on the one hand, and winter cooling on the other, determine the extent to which this basin supplies dense deep water and oxygen to the whole Mediterranean. In contrast, the South Aegean is one of the most oligotrophic areas in the Mediterranean Sea (Lykousis et al. 2002). The south Cretan margin (SCM) is part of the northern Levantine Sea proper. Surface water circulation is modulated by the effect of the Cretan gyre and is also affected by arid climatic conditions and fluctuations of the ITCZ and the monsoon/ENSO/Indian Ocean dipole system (e.g. Malanotte-Rizzoli et al. 1997).

High-resolution reconstructions in the Aegean marine records suggest that regional climate during the Holocene was less stable than previously thought (e.g. Rohling et al. 2002b; Emeis et al. 2003; Casford et al. 2003; Gogou et al. 2007; Kuhnt et al. 2007; Marino et al. 2007, 2009; Triantaphyllou et al. 2009a, b; Schmiedl et al. 2010; Katsouras et al. 2010; Kouli et al. 2012). These studies have mainly focused on time windows encompassing the S1 event. Mid-Holocene in the eastern Mediterranean represents a climatic transition between a wetter Early Holocene (deposition of sapropel S1) and a drier Late Holocene. Thus, the time period from 6 to 4 ka was not all wet or all dry, but included both wetter and drier phases of multi-centennial duration (Roberts et al. 2011a, b).

Detailed results for Mid-Holocene marine records are almost lacking in the eastern Mediterranean. Nevertheless, several continental records of the broader area document humid conditions during this time interval. Examples are a humid phase recorded during ~5.2–4.4 ka BP in the Dead Sea (Migowski et al. 2006) and the deposition of a sapropelic layer (upper sapropel layer; Tolun et al. 2002) in between 4.75 and 3.2 kyr uncal. BP in Marmara Sea, well above the equivalent of sapropel S1 in this basin, associated with the establishment of the dual flow regime between the Black Sea and the eastern Mediterranean (Çatağay et al. 2000). The paleorainfall calculated from the speleothem record of the Soreq Cave in Israel (Bar-Matthews et al. 2003; Bar-Matthews and Ayalon 2011) peaks between 4.8 and 4.7 ka, and in south-eastern Turkey Lake Van, a distinct wetter interval is centred at ~4.5 ka BP (Wick et al. 2003; Roberts et al. 2011a, b). In north Africa, humid conditions enabled the development of highly vegetated areas close to the Nile until ~4.5–4.0 ka BP (Lario et al. 1997). Additional evidence from Marathon coastal plain in eastern Greece (Pavlopoulos et al. 2006) implies warm, strongly seasonal climate from 5.8 to 3.5 ka BP. Reviewing several terrestrial data sets, Robinson et al. (2006) proposed a "Mid-Holocene wet event" at ~5.0 ka BP. Recently, the analysis of spatial distribution of several Mediterranean paleoclimatic records provided by Finné et al. (2011) identified the period between 6.0 and 5.4 ka BP as mainly wetter than average, followed by a decline in precipitation during the interval 5.4–4.6 ka BP. To date, a single marine core from the SE Aegean provides evidence for a warm/humid phase in the Mid-Holocene that is recorded in a sapropel-like layer deposited between 5.4 and 4.3 ka BP under stratified water column conditions and enhanced surface productivity (Sapropel Mid-Holocene (SMH), Triantaphyllou et al. 2009b).

Here, in order to further investigate the Mid-Holocene period in the eastern Mediterranean Sea after the sapropel S1 deposition 9 and 6 kybp, we address climate-driven environmental changes within the time window 6.0–2.5 ka BP (thus encompassing the SMH). Our specific aims are to (1) document the climate variability during Mid-Holocene in the marine archive and (2) assess the environmental

response of marine and terrestrial regimes to climate-driven environmental changes. For this purpose, we make high-resolution reconstructions from marine cores located along a latitudinal transect from the North Aegean Sea to the northern Levantine Sea (SCM), using a suite of marine and terrestrial biological and biogeochemical proxies (microfossils, pollen, organic carbon, $\delta^{13}C_{org}$, $\delta^{15}N$ and lipid biomarkers).

Materials and methods

Core descriptions

Core SL-152 (40°05.19′N, 24°36.65′E, water depth 978 m, length 670 cm) was recovered from the North Aegean Sea (Mount Athos basin) during RV Meteor cruise M51/3 in 2001 and comprises the last ~20 kyr (Fig. 1; Kotthoff et al. 2008b). Core NS-14 (36°38.55′N, 27°00.28′E, water depth 505 m, length 400 cm) was retrieved from the western Kos basin during RV Aegaeo cruise in 1998 and covers the last ~13 kyr (Fig. 1; Triantaphyllou et al. 2009b). Core HCM2/22 (34°33.97′N, 24°53.77′E, water depth 2,211 m, length 175 cm) was collected from the SCM in 2005 with the RV Aegaeo; the upper 60 cm covers the last ~20 kyr (Fig. 1; Ioakim et al. 2009). All cores feature a dark-coloured mud unit that corresponds to sapropel S1, consisting of two discrete intervals separated by a light-coloured interval, which corresponds to the S1 interruption. Detailed investigations of the S1 occurrence in these cores have been reported earlier (Kotthoff et al. 2008a; Triantaphyllou et al. 2009a, b; Katsouras et al. 2010). In core NS-14 (SE Aegean), the most recent Z2 Santorini ash layer is positioned at 17 cm depth, and a sapropel-like, dark olive grey mud layer (named Sapropel Mid-Holocene—SMH) is deposited between 25 and 40 cm and was described in detail in Triantaphyllou et al. (2009b).

Age models

The chronostratigraphy of the studied cores is based on eight accelerator mass spectroscopy (AMS) radiocarbon (^{14}C) dates available for core SL-152 (Kotthoff et al. 2008a, b), seven for core NS-14 (Triantaphyllou et al. 2009b) and three for core HCM2/22 (Ioakim et al. 2009; Katsouras et al. 2010). The dates of all cores used in this study have been calibrated using a regional marine reservoir correction of 58 ± 85 years (Reimer and McCormac 2002) for non-sapropel and 149 ± 30 years (Facorellis et al. 1998) for sapropel intervals. The age model of NS-14 (Triantaphyllou et al. 2009b) has been tested against the multi-proxy chronological framework proposed by Casford et al. (2007). All ages in this study refer to calibrated ^{14}C ages.

During the last 6.0 kyrs, sedimentation rates (SRs) in core SL-152 reach ~39 cm/kyr, a high rate even for the North Aegean Sea, where generally SRs are ~20 cm/kyr (Roussakis et al. 2004). In the SE Aegean, SRs fluctuate around 13 cm/kyr (NS-14), similar to earlier estimates for this region (Lykousis and Chronis 1989; Piper and Perissoratis 1991; Roussakis et al. 2004). At the SCM site (core HCM2/22), SRs are as low as ~3 cm/kyr, typical of the open eastern Mediterranean Sea (Emeis et al. 2000).

Methods

Micropaleontological proxies: coccolithophores and dinoflagellates

Preparation of samples, quantitative counting methods and taxonomy of coccolithophore analysis are described in detail in Triantaphyllou et al. (2009a, b). The lower photic zone species *Florisphaera profunda* has proven to be a reliable proxy of the nutricline–thermocline (Okada and Honjo 1973; Molfino and McIntyre 1990); thus, high relative abundances indicate stable stratification of the water column and low productivity in the surface layer (e.g. Castradori 1993; Beaufort et al. 2001; Flores et al. 2000). *Emiliania huxleyi* is considered to be a proxy for high nutrient concentrations in surface waters (Young 1994) and is a species that prevails during winter in the Aegean Sea (Dimiza et al. 2008). *E. huxleyi* moderately calcified morphotypes (EHMC) indicate low surface temperatures as they are restricted to cool Holocene intervals (Crudeli et al. 2006) and mark the present-day winter season in the Aegean (Dimiza et al. 2008; temperatures >16 °C, Poulos et al. 1997). Relative maxima in the abundances of *Helicosphaera* spp. (mainly *Helicosphaera carteri*) and *Syracosphaera* spp. together with *Braarudosphaera bigelowii* have been used as indicators of salinity decrease, whereas *Rhabdosphaera* spp. signal stratified and oligotrophic upper water column layers (e.g. Triantaphyllou et al. 2009a, b).

Dinoflagellate cyst data were raised on cores NS-14 and HCM2/22. Preparation techniques, taxonomy and quantitative counting methods are described in Triantaphyllou et al. (2009a) and Geraga et al. (2010). Heterotrophic species susceptible to post-depositional oxidation (e.g. *Stelladinium* spp., *Selenopemphix* spp., *Selenopemphix nephroides*, *Selenopemphix quanta*, *Lejeunecysta* spp.; Zonneveld et al. 2007) have been recorded in core NS-14, where their fluctuations in relative abundance largely follow those of autotrophs (e.g. *Spiniferites mirabilis*, *Spiniferites hyperacanthus*, *Lingulodinium machaerophorum*, *Nematosphaeropsis labyrinthus*, *Operculodinium centrocarpum* sensu Wall & Dale, *Operculodinium israelianum*, *Polysphaeridium zoharyi*, *Pyxidinopsis reticulata*, *Impagidinium aculeatum*, *Impagidinium patulum, Impagidinium*

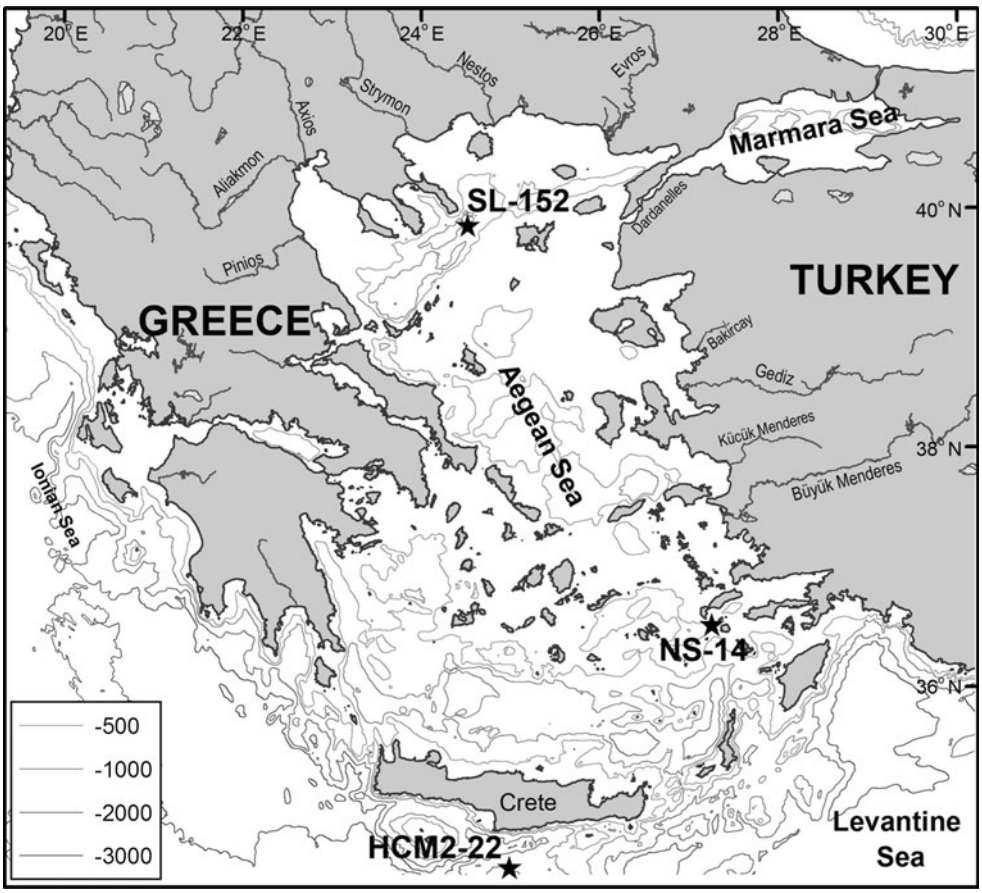

Fig. 1 Location *map* of the Aegean and northern Levantine Seas, showing the locations of the studied sites, the bathymetry and the rivers

paradoxum, Pentapharsodinium dalei). This suggests that oxidation effects on preserved dinoflagellate assemblages are not significant and implies that increases in heterotroph abundances likely reflect higher productivity.

Pollen records

Pollen records from cores NS-14, HCM2/22 and SL-152 have been previously reported (Triantaphyllou et al. 2009a, b; Kotthoff et al. 2008a, b; Kouli et al. 2012). Here, pollen data are summarized, and only selected groups are presented. *Pinus* is not included in the "conifers" data. "Mediterranean taxa" include *Cistus, Phillyrea, Pistacia, Ligustrum* and *Olea,* while *Quercus ilex* has been plotted separately. Non-arboreal pollen (NAP) is given as a sum.

TOC, $\delta^{13}C_{org}$, $\delta^{15}N$, marine and terrestrial biomarkers

Methods and results for total organic carbon (TOC) content and $\delta^{13}C_{org}$ have been previously reported in detail (Katsouras et al. 2010). $\delta^{15}N$ was determined following the same methodology using a Thermo 1500 elemental analyzer coupled to a Finnigan MAT 252 continuous-flow gas isotope ratio mass spectrometer for cores SL-152 and NS-14, and a PDZ Europa ANCA-GSL elemental analyzer coupled to a PDZ Europa 20–20 IRMS instrument for core HCM2/22. Stable carbon and nitrogen isotope ratios (R) are expressed as $\delta^{13}C$ and $\delta^{15}N$ values against V-PDB for carbon and atmospheric N_2 for nitrogen. The overall analytical error based on duplicate measurements was ±0.2 ‰ for $\delta^{13}C$ values and ±0.3 ‰ for $\delta^{15}N$ values.

Lipid biomarkers in core SL-152 were analysed following the methods described in Gogou et al. (2007). Methods and data for cores NS-14 and HCM2/22 were published in Triantaphyllou et al. (2009b) and Kouli et al. (2012). Individual compounds were identified and quantified by GC–FID and GC–MS. Here, we report as marine biomarkers the sum of $C_{27} + C_{28} + C_{30}$ algal sterols, C37 + C38 long-chain alkenones and diols-keto-ols, whereas the sum of long-chain *n*-alkanols and *n*-alkanes represents terrestrial biomarkers. The sum of loliolide and isololiolide is presented separately. The initial results expressed as concentrations (ng/g) were converted to accumulation rates (ARs), calculated using absolute biomarker concentrations (ng g^{-1} dry sediment), linear sedimentation rates (LSR, cm/kyr) and dry bulk density of the sediment (g/cm^3).

Alkenone-based sea surface temperatures (SSTs) and paleoceanographic/paleoclimatic indices

Past sea surface temperatures (SST) for cores SL-152 and HCM2/22 were estimated from unsaturation ratios of alkenones ($U^{k'}_{37}$) and the global calibration given by Müller et al. (1998). The analytical precision based on multiple extractions of sediment samples was better than 0.6 °C. The results are here compared with alkenone-based estimates of SST in core NS-14 (Triantaphyllou et al. 2009b).

The ratio of the abundances of terrestrial *n*-alkanes and *n*-alkanols (HPA index = [Ter-alkanols]/([Ter-alkanols] + [Ter-alkanes]); Poynter and Eglinton 1990) is used to evaluate stratification/oxygen depletion in the marine water column that promotes in situ preservation (Versteegh et al. 2010; Kouli et al. 2012). Changes in the vegetation cover during different climatic periods could be inferred by changes in the average chain length of terrestrial *n*-alkanes (ACL index, e.g. Zhou et al. 2010; Kouli et al. 2012).

Estimates of coccolithophore net primary production (NPP) in the upper part of the water column are based on Incarbona et al. (2008). In addition, the relative intensity of mid-water stratification is estimated from the ratio *S* (*S* index; Triantaphyllou et al. 2009b) between *F. profunda* (*F*) and *E. huxleyi* (*E*) abundances: $S = F/(F + E)$.

Two different pollen ratios are used here as paleoenvironmental proxies. The ratio H = AP/St (AP: arboreal taxa excluding *Pinus*; St: steppic taxa including *Artemisia*, Chenopodiaceae, Asteraceae and Poaceae) has been suggested as a humidity index (*H* index; Triantaphyllou et al. 2009b). The forestation cover index that expresses the expansion of broadleaved forest in adequate moisture conditions (Kotthoff et al. 2008b; Kouli et al. 2012) has been calculated based on the ratio of broadleaved taxa (*Acer*, *Alnus*, *Betula, Cistus, Corylus, Fagus, Fraxinus, Juglans, Olea, Phillyrea, Pistacia, Platanus, Populus, Ostrya, Quercus, Tilia, Ulmus*) to pollen sum excluding bisaccates.

The temperature index warm/cold (W/C) for core NS-14 is derived from the warm-water dinocyst assemblage *Tuberculodinium vancampoae, Tectatodinium pellitum, S. nephroides, I. patulum, I. aculeatum, Pyxidinopsis reticulata, O. israelianum, Spiniferites mirabilis, S. hyperacanthus,* and the cold-water assemblage *N. labyrinthus, P. dalei.* The W/C index for core HCM2/22 is derived from the warm-water assemblage *I. aculeatum, I. patulum, Spiniferites bentorii, S. mirabilis, S. hyperacanthus* and the colder-water assemblage, *N. labyrinthus, Spiniferites elongatus*.

Results

The individual sediment sequences and inferred paleoenvironmental conditions for the whole Holocene in cores SL-152, NS-14 and HCM2/22 have been published (Kotthoff et al. 2008a, b; Triantaphyllou et al. 2009a, b; Katsouras et al. 2010; Kouli et al. 2012). Here, we provide an integrated paleoenvironmental reconstruction for the time window from 6.0 to 2.5 ka BP from the three cores.

Coccolithophores

In the North Aegean location (core SL-152), *E. huxleyi* relative abundance is drastically lower (down to ~10 %) between 5.5 and 4.0 ka BP compared to the interval younger than 4.0 ka BP, where it reaches 60 % (Fig. 2). EHMC morphotypes show significantly higher values before 4.9 ka BP and between 4.0 and 2.5 ka BP. In contrast to *E. huxleyi, F. profunda* displays high abundances (60 and 90 %) between 5.5 and 4.0 ka BP, whereas *Helicosphaera* spp., *Syracosphaera* spp. and *Rhabdosphaera* spp. are minor contributors. *B. bigelowii* is present, although in low abundance, throughout the interval between 6.0 and 3.0 ka BP.

The SE Aegean core NS-14 displays *E. huxleyi* oscillations (40–60 %) with two distinct minima (40 %) centred on 6.0 and 4.8 ka BP (Fig. 2). EHMC morphotypes present a distinct maximum in abundance centred on 3.5 ka BP. *F. profunda* increases at 4.8 ka BP. An interval with high abundances of *Helicosphaera* spp. and *Rhabdosphaera* spp. occurs between ~5.5 and 4.0 ka BP. *B. bigelowii* is present in low abundances up to 4.6 ka BP (Fig. 2).

In core HCM2/22 on the southern margin of Crete, *E. huxleyi* relative abundance initially peaks at 70 %, but then falls below 40 % at ~4.5 ka BP. EHMC cold morphotypes show maximum abundance after 4.0 ka BP. In contrast, *F. profunda* abundance remains relatively low after 6.0 ka BP (Fig. 2) and increases to 40 % at ~4.5 and 2.0 ka BP. *Rhabdopshaera* spp., *Helicosphaera* spp. and *Syracosphaera* spp. show similar patterns as *F. profunda*, whereas *B. bigelowii* peaks at ~6.5 ka BP.

Dinoflagellates

Dinoflagellate data are not available for core SL-152. The dinoflagellate record (Fig. 3) from SE Aegean core NS-14 reveals overall low abundances and displays increased relative percentages of heterotrophs (such as *Stelladinium reidii, Selenopemphix quanta* and *S. nephroides*) from 5.4 to 4.3 ka BP. Of the autotrophic taxa, the inner neritic *L. machaerophorum* is slightly more abundant in samples dated between ~5.0 and 4.0 ka BP.

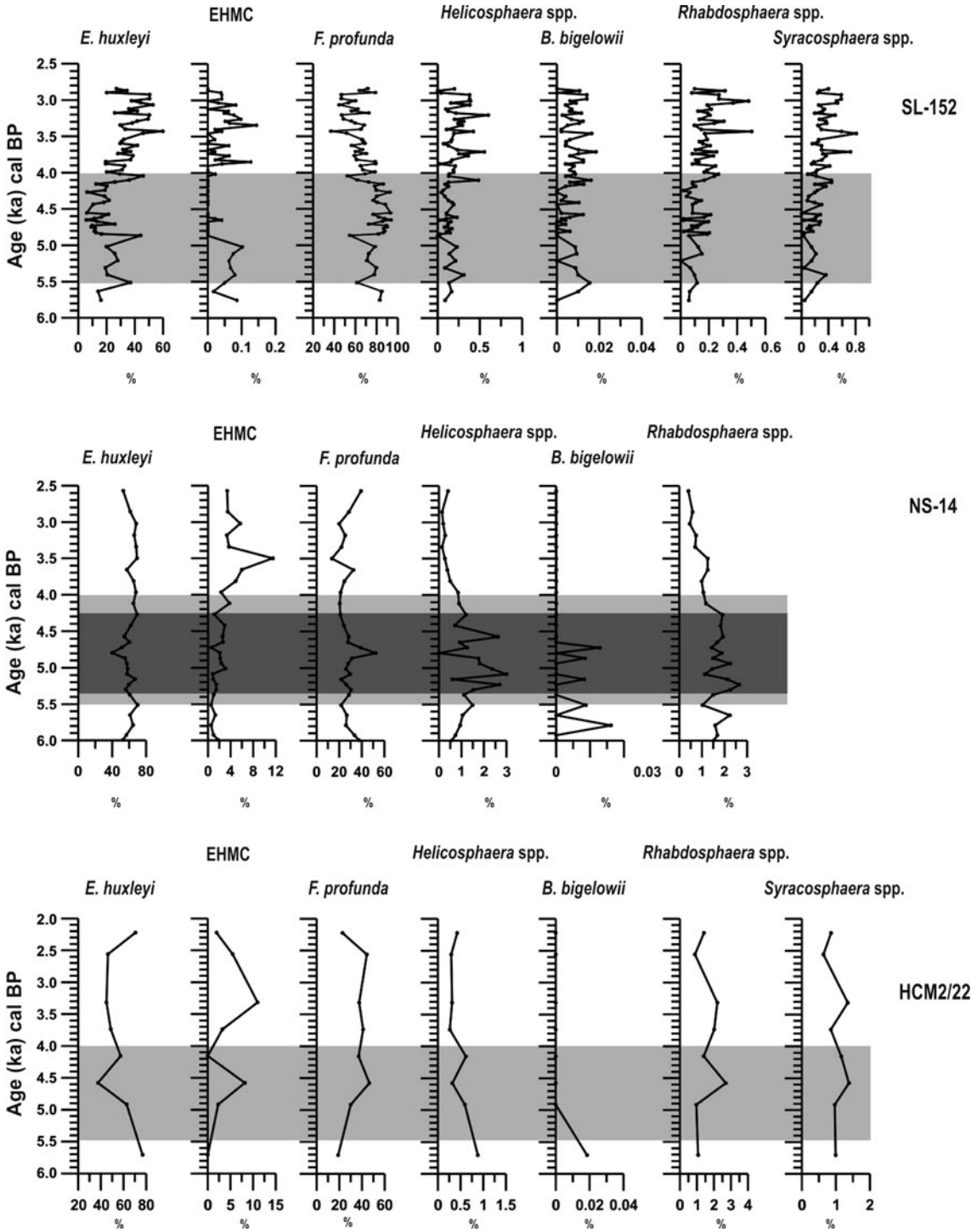

Fig. 2 Relative abundance of coccolithophore species for cores SL-152, NS-14 and HCM2/22 expressed in percentage. The *darker grey* in NS-14 represents the SMH sapropelic layer

The heterotrophic component is barely present in the dinocyst record of northern Levantine core HCM2/22 (Fig. 3). However, a rare occurrence of the heterotrophic cyst *Brigadentinium simplex* is recorded at 4.5 ka BP.

Pollen records

Pollen spectra (Fig. 4) of SL-152 feature decreasing conifer abundances after 5.2 ka BP, while *Quercus* and other deciduous taxa have high abundances after 5.4 ka BP.

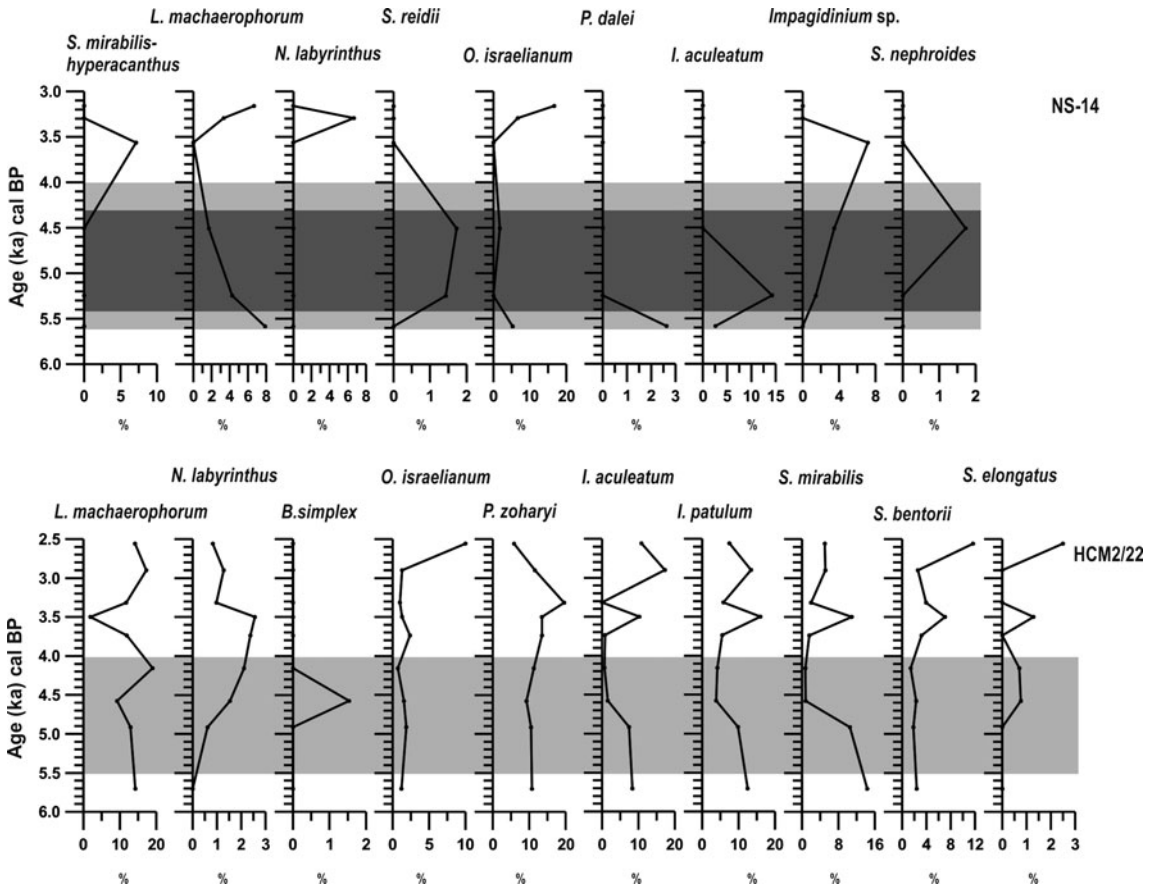

Fig. 3 Relative abundance of dinoflagellate species for cores NS-14 and HCM2/22 expressed in percentage. The *darker grey* in NS-14 represents the SMH sapropelic layer

Mediterranean taxa (excluding evergreen *Quercus*) are minor contributors to the pollen assemblages, but their abundances increase between 4.7 and 4.0 ka BP and from 3.2 to 2.7 ka BP. NAP abundances are low around 5.3 ka BP.

In the SE Aegean NS-14 record, abundances of Mediterranean taxa (excluding *Quercus*) are low between 5.2 and 4.3 ka BP and have an increasing trend after 4.0 ka BP. A similar pattern is observed in the NAP record, which has the lowest relative contributions to the total pollen around 5.0 ka BP. Conifers and deciduous *Quercus*, though fluctuating, distinctly increase between 5.3 and 4.5 ka BP (Fig. 4), whereas the abundance of conifer pollen decreases from 4.2 ka BP onwards.

Herb vegetation and Mediterranean taxa, mainly represented by evergreen *Quercus*, dominate the HCM2/22 pollen spectra in sediments younger than 6.0 ka BP and contribute 42 and 12.5 % to the assemblage, respectively. Deciduous taxa decrease after 4.3 ka BP, while NAP abundance increases (Fig. 4).

TOC, $\delta^{13}C_{org}$, $\delta^{15}N$, marine and terrestrial biomarkers

In the North Aegean SL-152 record, TOC and $\delta^{13}C_{org}$ values vary in narrow ranges, from 0.5 to 0.55 % and from −22.4 to −21.6 ‰, respectively, while $\delta^{15}N$ values show relatively higher variability [∼1–4 ‰ (Fig. 5)]. Between ca. 5.5 and 5.0 ka BP, TOC exhibits a slight increase while $\delta^{13}C_{org}$ shifts to less-negative values and is relatively constant thereafter. $\delta^{15}N$ exhibits minimum values at ∼5.5 ka BP, followed by a positive shift from 5.3 to 4.3 ka BP and a slight decrease afterwards. ARs of terrestrial biomarkers increase at ∼5.5 and fluctuate until ∼5.0 ka BP, with lower ARs after that time (Fig. 5). ARs of marine biomarkers exhibit several positive shifts in the interval 5.5–4.0 ka BP.

In core NS-14, a relative increase in TOC values (slightly exceeding 0.8 %) occurs in the interval 5.4–4.3 ka BP. The $\delta^{13}C_{org}$ values show a prominent increase, peaking at ∼4.9 ka BP, in contrast to a decreasing trend of $\delta^{15}N$ values that have a minimum at ∼4.6 ka BP. Elevated ARs of marine biomarkers are observed from 5.4 to 4.3 ka BP

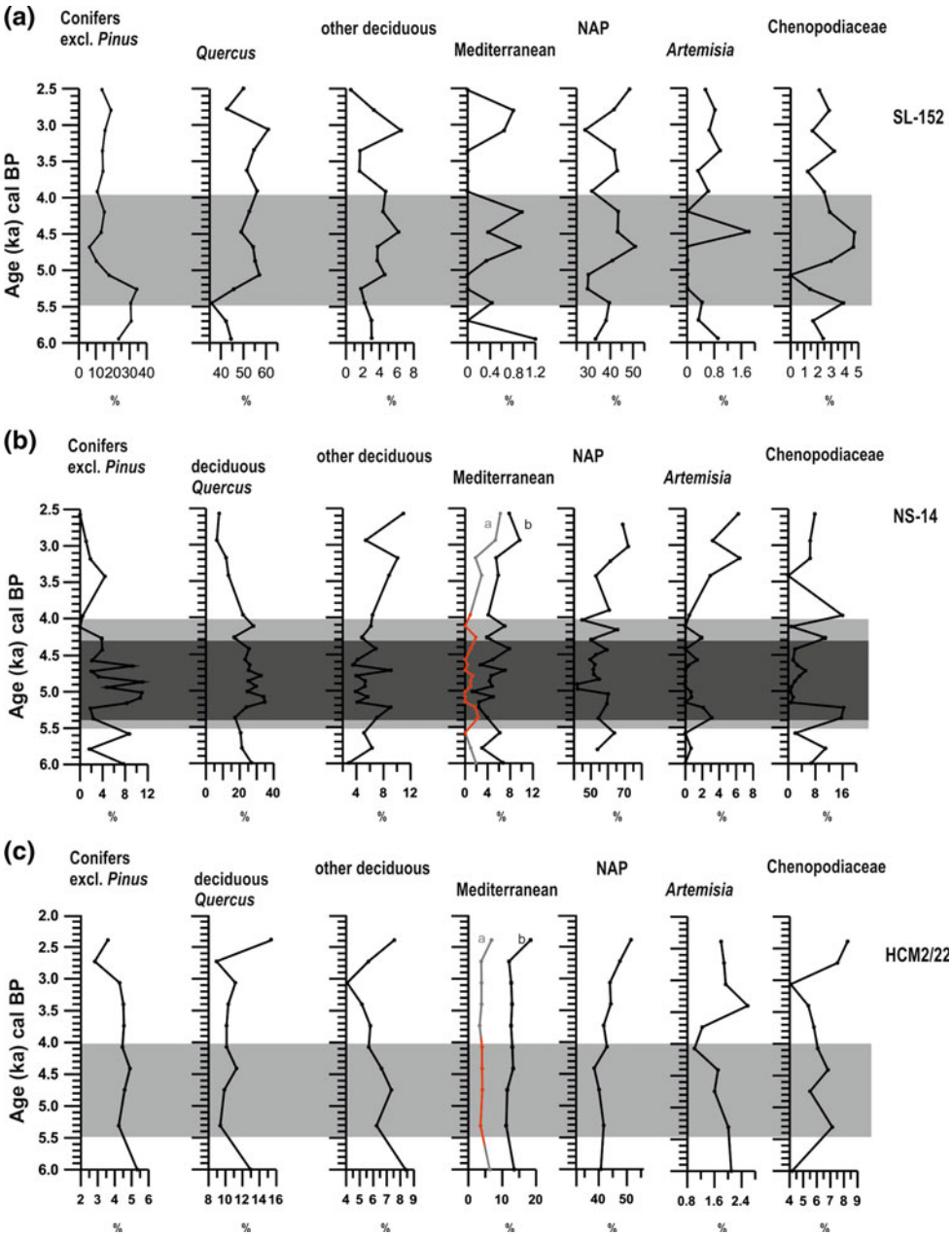

Fig. 4 Percentages of the most indicative pollen groups in cores SL-152 (**a**), NS-14 (**b**), and HCM2/22 (**c**). Conifers include *Abies, Cedrus* and *Picea*; deciduous taxa include *Acer, Alnus, Betula, Carpinus, Corylus, Fraxinus, Juglans, Tilia* and *Ulmus*. Mediterranean taxa are presented in two curves in cores NS-14 (**b**) and HCM2/22 (**c**): **a** including *Olea, Ligustrum, Phillyrea* and *Pistacea*, while in **b** evergreen *Quercus* is also integrated. In core SL-152, deciduous and evergreen *Quercus* are plotted together and Mediterranean taxa include *Olea, Ligustrum, Phillyrea* and *Pistacea*. The *darker grey* in NS-14 represents the SMH sapropelic layer

(av. ARs 18.5 and 41.5 ng cm^{-2} kyr^{-1}, respectively). During the same interval, loliolide and isololiolide ARs are high (av. ARs 11 ng cm^{-2} kyr^{-1}; Fig. 5). Similar to the patterns of TOC and marine biomarkers, terrestrial ARs are elevated (110 and 94 ng cm^{-2} kyr^{-1}, respectively), and the HPA index maximises at ~5.0 ka BP (0.8; Fig. 5).

In the HCM2/22 record, TOC concentrations are low between 5.5 and 4.0 ka BP (0.23–0.26 %; Fig. 5). The three samples analysed for $\delta^{13}C_{org}$ and $\delta^{15}N$ values have narrow ranges from −22.5 to −21.5 ‰ and from 4 to 5 ‰, respectively. ARs of marine biomarkers are also very low in comparison with those of the corresponding time intervals in cores NS-14 and SL-152 and are not markedly higher from 4.7 to 5.3 ka BP (Fig. 5). Although at low values compared to the Aegean sites and varying significantly amongst samples, terrestrial biomarkers appear to accumulate at slightly higher rates during the 6.0–2.5 ka BP interval; the HPA index peaks at ~4.7 ka BP with a value of 0.4 (Fig. 5).

Alkenone-based sea surface temperatures (SSTs) and paleoceanographic/paleoclimatic indices

SSTs in core SL-152 decline steadily from 19 °C at 6.0 ka BP to 15 °C at 2.5 ka BP, with some variability between 5.5 and 4.0 ka BP (Fig. 6). The stratification *S* index varies

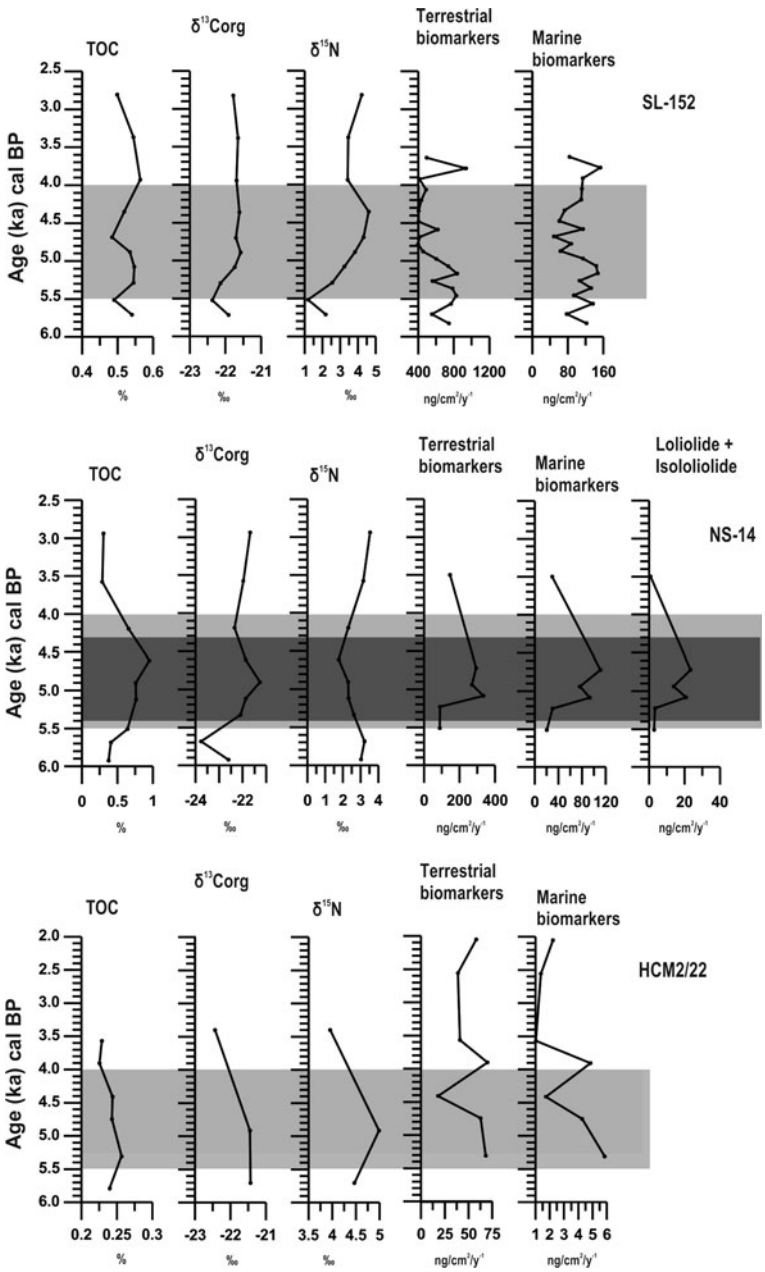

Fig. 5 TOC (%), $\delta^{13}C_{org}$ (‰), $\delta^{15}N$ (‰) and accumulation rates (ARs) of the investigated terrestrial and marine biomarkers for cores SL-152, NS-14 and HCM2/22. The *darker grey* in NS-14 represents the SMH sapropelic layer

between 0.6 and 0.9 and has a distinct positive shift at ~5.0 ka BP. The calculated net primary production (NPP) is low and increases steadily towards younger samples, clearly anticorrelated with the *S* index. The *H* index exhibits two maxima between 5.4 and 5.0 ka BP and a third maximum at ca. 3.0 ka BP. The forestation cover index has a temporal pattern similar to the *H* index, whereas HPA and ACL indices exhibit several positive shifts.

In the NS-14 record, SSTs (Fig. 6) are higher than 20 °C in samples younger than 6.0 ka BP, with an average value of 22 °C between 5.4 and 4.3 ka BP and a prominent positive excursion to 24.9 °C at ~4.9 ka BP. The dinoflagellate-derived W/C index also displays an increasing trend (Fig. 6). Temperature falls to 18.5 °C at ~3 ka BP, similar to the values calculated in the North Aegean (Gogou et al. 2007). The stratification *S* index peaks (~0.6) at 4.8 ka BP (Fig. 6), while NPP shows an inverse trend. The ACL, forestation cover and *H* indices are highest from 5.2 to 4.7 ka BP and around 4.1 ka BP (reaching 2.4, 30.2 and 0.54, respectively) (Fig. 6).

In core HCM2/22, a very low abundance of alkenones did not allow for SSTs reconstructions for the last 6.0 ka BP. The main positive shift of the *S* index (0.6) occurs at ~4.5 ka BP, coupled to a minimum in the NPP index that

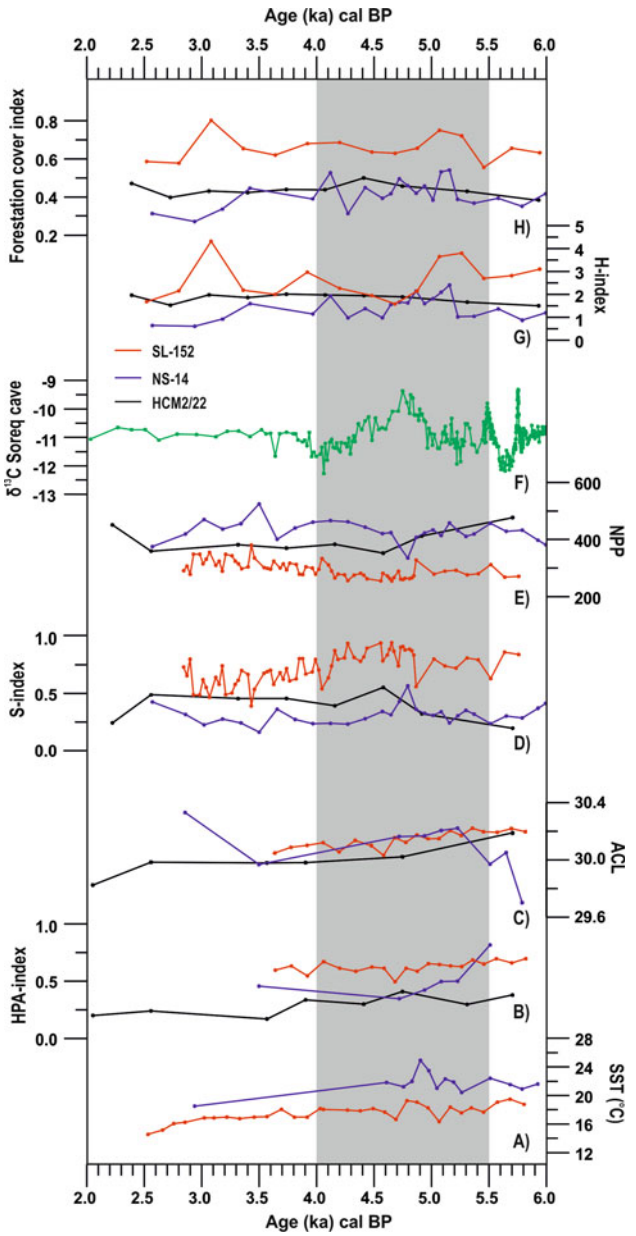

Fig. 6 Comparison of paleoceanographic indices for cores SL-152, NS-14 and HCM2/22 with the Soreq cave, Israel, record (from Almogi-Labin et al. 2009 and Bar-Matthews and Ayalon 2011) during the 5.5–4.0 ka BP time interval. *a* Alkenone-based sea surface temperatures (SST), *b* terrestrial HPA index, *c* average chain length of terrestrial *n*-alkanes ACL index, *d* coccolithophore stratification *S* index, *e* upper water column net primary productivity (NPP), *f* Mid-Holocene $\delta^{13}C$ data from Soreq cave, *g* pollen humidity *H* index, *h* forestation cover index

reaches ~350 in the same interval. While the ACL and *H* index show no conspicuous features (mean 1.8), the forestation cover index exhibits increased values (mean 30.0 and 0.45) between ~5.4 and 4.3 ka BP. The dinoflagellate-based temperature W/C index suggests warm sea surface conditions from 5.7 to 4.9 ka BP and a cool episode centred at 4.1 ka BP (Fig. 6).

Discussion

Regional paleoceanographic and paleoclimatic implications

Humidity and freshwater influx

Between ~5.5 and 4.0 ka BP in the North Aegean SL-152 core record, the continuous presence of low-salinity indicator coccolithophore species *Helicosphaera* spp. and *B. bigelowii* (Fig. 2) shows increased supply of freshwater. This is consistent with the planktonic $\delta^{18}O$ record of nearby core SL-148 until approximately 4.3 ka BP (Kuhnt et al. 2007), coinciding with the maximum of the Black Sea influence reported by Sperling et al. (2003). A similar pattern of *Helicosphaera* spp. was evidenced in the SE Aegean core NS-14 (Fig. 2), supporting lower salinities within the regional SMH depositional interval (Triantaphyllou et al. 2009b). This is further supported by the low percentages of the oceanic species *Impagidinium* spp. and by higher percentages of the inner neritic and euryhaline species of *L. machaerophorum* at the lower part of the SMH layer (Fig. 3). Following the same pattern, *Helicosphaera* spp. shows a positive shift at ~4.5 ka BP in the northern Levantine SCM core HCM2/22 (Fig. 2).

Notably, increased pollen-based indices (forestation cover and *H* indices) in the Aegean and northern Levantine Seas (Fig. 6) record a brief expansion of forest cover after ~5.5–5.0 ka BP, which is attributed to an increase in humidity. This humid period interrupts an aridification trend, featured by weakening of the seasonal contrast of precipitation that ended at ~5.0 ka BP (Peyron et al. 2011). Similar patterns have been recorded also in other marine sites in the Aegean region (Geraga et al. 2000, 2010; Kouli et al. 2012). Nevertheless, the forest cover in the northern borderlands of the Aegean Sea was not as dense as during the moist conditions of the Early Holocene (Kotthoff et al. 2008a, b). Although this demise of dense forests could be due to an increasing anthropogenic land use (Lespez 2003), recent studies (Sadori et al. 2011) proposed that climatic variability was the main cause of the vegetation changes recorded before ~4.0 ka BP, even if locally restricted human activity can be detected in terrestrial records. The recorded humid period in the SL-152 pollen dataset is bracketed by a centennial-scale drought event centred at ~5.5 ka that coincides with the regional weakening of monsoonal rainfall in northern Africa (e.g. Gasse and van Campo 1994; de Menocal et al. 2000) and a multicentury drought event between ~4.7 and ~4.1 ka BP (Kotthoff et al. 2008a, b). This is clearly recorded by the decreasing percentages of arboreal pollen followed by an increase in steppe element *Chenopodiaceae* (Fig. 4). Strong inputs of land-derived material in the study site are

also evidenced by a peak of terrestrial biomarker ARs at ~5.2 ka BP (Fig. 5). Similarly, increasing trends of the pollen-derived humidity *H* index are observed in the southern North Aegean MNB-3 record centred at ~4.5 ka BP and are accompanied by an increase in the warmer vegetation type (Geraga et al. 2010; Kouli et al. 2012). The enhanced continental run-off is also evident at the SE Aegean NS-14 site, with high aquatic palynomorph concentrations and higher accumulations of terrestrial biomarkers during ~5.3–4.7 ka BP (Triantaphyllou et al. 2009b), whereas pollen evidence includes an expansion of deciduous forest elements and an amplified humidity *H* index (Fig. 6). Further evidence of higher humidity during the Mid-Holocene at the SCM (HCM2/22) is provided by the simultaneous increase in the forestation cover index (Fig. 6). In support to this change, noticeable increases in the ARs of terrestrial biomarkers (Fig. 5) and the HPA index values centred at ~4.7 ka BP indicate enhanced terrigenous inputs of organic matter along with better in situ preservation (Kouli et al. 2012). Furthermore, positive shifts in the ACL index at this time, particularly in northern and SE Aegean records (Fig. 6), are in accordance with the climate-induced vegetation change deduced from palynological analyses, marking a vegetation shift towards species indicative of warmer and probably wetter conditions (Zhou et al. 2010; Kouli et al. 2012).

Sea surface temperature

EHMC are practically absent during ~5.0–4.0 ka BP in the SL-152 and show low abundances in SE Aegean and SCM data sets, thus indicating higher surface temperatures (Fig. 2). Adding to this evidence, Geraga et al. (2010) identified an interval of warm and productive surface waters in the central Aegean between 5.0 and 3.0 ka based on planktonic foraminifers and dinocyst concentrations. Consistent with the EHMC pattern, the dinocyst-derived W/C ratio from the HCM2/22 and NS-14 records also reveals maximum SST around 4.9 ka BP (Fig. 6).

The biogenic evidence for warm conditions agrees with alkenone SST estimates that suggest warming to 19 °C at ~4.8 ka BP in the North Aegean and a sharp positive shift to 24.9 °C at ~4.8 ka BP in the SE Aegean Sea (Fig. 6). Notably, the estimated SSTs in the SE Aegean, although fluctuating, never fall below 22 °C between ~6.0 and 4.0 ka BP, indicating continually relatively warm conditions during the Mid-Holocene. This may mirror the inferred dominance of warmer Levantine waters within 5.5–4.0 ka BP (Rohling et al. 2002a, b; Marino et al. 2009) in the southern Aegean Sea. As in the Aegean Sea, warming has been reported at ~5 ka BP for the southern Adriatic Sea (Emeis et al. 2000; Giunta et al. 2003; di Donato et al. 2008).

SSTs have not been calculated in the SCM record due to its low alkenone contents. However, available $U^{k'}_{37}$ SST reconstructions in the eastern Mediterranean (Ionian Sea, Nile delta) show warm conditions during the Mid-Holocene interval from ~5.0 to 4.0 ka BP (Emeis et al. 2000; Castañeda et al. 2010).

Upper water column stratification and productivity

The warm and humid climatic conditions that prevailed during 5.5–4.0 ka BP had a profound impact on the water column features. The higher relative abundance of *F. profunda* and the elevated coccolithophore stratification *S* index (0.6–0.9) in the North Aegean (0.5–0.8) in SE Aegean and with a main shift to 0.6 at SCM (Fig. 6) indicate stable stratification in the upper water column and increased productivity in the lower photic zone. Furthermore, the shift of $\delta^{13}C$ towards higher values (~−21.5 ‰; Fig. 5) and a relative increase in marine biomarker ARs are consistent with elevated marine productivity, probably reflecting enhanced organic matter inputs of algal/marine origin at all sites during this time period (e.g. Gogou et al. 2007; Katsouras et al. 2010).

Interestingly, the *S* index values and *F. profunda* abundances reveal relatively stronger stratification of the water column and an enhanced DCM in the North Aegean compared to the other sites, where upper water column productivity (NPP) is considerably higher (Fig. 6). This occurs because the northern site was under the influence of increased freshwater supply from the nearby river systems of the southern Balkans and the Black Sea catchment; Black Sea outflow, although subordinate to the river discharging of the North Aegean Sea (Ehrmann et al. 2007), initiated between 8.0 and 7.0 ka BP and reached its maximum at around 5.0–4.0 ka BP (Sperling et al. 2003).

Sea-floor conditions and preservation

Triantaphyllou et al. (2009b), using benthic foraminifera assemblages and loliolide-isololiolide ARs, showed that the SE Aegean NS-14 core records dysoxic conditions at the water column–sediment interface during 5.4–4.3 ka BP that are evidenced by the formation of the SMH layer. In addition to this, the pattern of $\delta^{15}N$ shows a slight decrease at ~4.6 ka BP (Fig. 5), indicating a more significant contribution from nitrogen-fixing organisms, similar to the trend recorded under higher productivity sapropel deposition events (Gallego-Torres et al. 2011 and references therein) and/or better preservation of the $\delta^{15}N$ signal under low-oxygen conditions (Möbius et al. 2010).

For the two sites in the North Aegean (SL-152) and the SCM (HCM2/22), we can exclude dysoxic conditions in

the 5.5–4.0 ka BP time interval: low TOC concentrations (Katsouras et al. 2010), low ARs of marine and terrestrial biomarkers, and elevated δ^{15}N values (Fig. 5) together indicate that the deep North Aegean and the northern Levantine Sea SCM were fully oxygenated. Thus, a top–down mechanism of stratification–DCM development–fast transport and burial of organic matter is the most reasonable explanation for the preservation of productivity signal in shallow sites, leading to sapropelic conditions during the warm and humid Mid-Holocene. This is clearly opposed to sapropel S1 mode as has been claimed previously (e.g. Emeis et al. 2000; Casford et al. 2003; Katsouras et al. 2010), where the deeper basins were isolated first, due to the development of severe stratification that led to the isolation of deep-water masses and the establishment of extended anoxia at the water column–sediment interface.

Regional versus long-termed Mid-Holocene climate variability

The Mid-Holocene period (6.0–2.5 ka BP) in the eastern Mediterranean region is a time interval of intensifying human activity, resulting in the foundation and transformation of complex societies (e.g. Finné et al. 2011). From the paleoclimatic perspective, it represents a period when the redistribution of solar energy due to orbital forcing on a millennial timescale resulted in a progressive decrease in Northern Hemisphere (NH) insolation and southward shift of the NH summer position of the ITCZ (e.g. Gasse 2000). According to Zhou et al. (2010) and Magny et al. (2009, 2012), the climate change around 4.5 ka BP was possibly caused by large-scale changes in atmospheric circulation, linked to a non-linear response of the climate system to the gradual decrease in insolation. Roberts et al. (2011a) documented a see-saw effect between eastern and western Mediterranean basins during the Mid-Holocene transition, with less precipitation in the eastern basin after ~6 ka BP. However, high-resolution studies (e.g. Soreq Cave, Israel, Bar-Matthews and Ayalon 2011) are consistent with sinusoidal cycles between wetter and drier climate during the Mid-Holocene, in accord with Bond events. In particular, Bar-Matthews and Ayalon (2011) noticed several wet periods, including the 4,800–4,700-yr BP event that coincides with the transition from early Bronze II to early Bronze III cultural change. A direct comparison of our records with the high-resolution Mid-Holocene δ^{13}C data from Soreq cave verifies the wet climate conditions that prevailed during the Mid-Holocene and associated with the SST increase in Aegean Sea (Fig. 6).

Tinner et al. (2009) pointed out that the Mid-Holocene increase in humidity in the southern Mediterranean probably reflects a decrease in the Hadley circulation and monsoonal activity that weakened the north Atlantic anticyclone and unblocked possible intrusion of western humid airflow towards the Mediterranean (Gaetani et al. 2007). Adding to this, our evidence for warm and humid Mid-Holocene conditions in the Aegean and northern Levantine Seas may also be the result of ongoing, albeit weak, Mid-Holocene South Asian monsoon forcing (Thamban et al. 2007) combined with lighter northerly winds (Etesians) in the Aegean, as the actualistic contemporary model presumes (Tyrlis et al. 2012). This led to reduced upwelling, therefore supporting an increase in the stratification of the water column and the localized formation of SMH in the sensitive site of SE Aegean Sea. Recent studies connect the abrupt fluctuations in the Asian summer monsoon with the North Atlantic climate (Gupta et al. 2003, 2005; Wang et al. 2005), which may be linked to abrupt reorganizations of the thermohaline circulation. Specifically, for the Mid-Holocene, a retreat of southern Scandinavian glaciers is recorded (Lie et al. 2004; Wanner et al. 2008), and more recent data from west Greenland (Perner et al. 2012) indicate a prolonged warm phase between 5.5 and 3.5 ka BP, which is probably associated with the large-scale variability of the North Atlantic Current.

The termination of the Mid-Holocene warm and humid phase corresponds with the reduction in the rate of sea-level rise at ~4.0 ka BP in the Aegean Sea (Pavlopoulos et al. 2011) and the concomitant evolution of Aegean coastal plains (Koukousioura et al. 2011). In a broader sense, the end of warm and wet conditions coincides with the NH rapid climate cooling at 4.2 ka (Mayewski et al. 2004), which is also expressed in the Adriatic Sea (Piva et al. 2008), and central Mediterranean lake records (Magny et al. 2009). This dry and cool episode is evidenced at low latitudes as a "mega-drought event" between ~4.5 and ~4.0 ka BP (Cullen et al. 2000) that may have resulted to the fall of the Egyptian Old Kingdom and the collapse of Akkadian Empire (e.g. Weiss et al. 1993; Gasse and van Campo 1994; Gasse 2000). Barring age model uncertainties, our humidity evidence suggest that aridification began at ~5.0 ka BP in the North Aegean versus ~4.7 ka in the SE Aegean, consistent with the north–south trend over the Holocene period. The northern Mediterranean borderlands belong to a north Atlantic domain with strong similarities with European mid-latitudes (Magny et al. 2011, 2012), while the southern Mediterranean borderlands appear to be more affected by sub-tropical climatic patterns. The persistence of humid conditions in the southern parts of the Aegean Sea is most probably associated with the reorganization of the general atmospheric circulation during the Mid-Holocene. This gradual establishment of arid conditions in the area may complicate the recognition of the "4.2 ka" as a distinct event in the eastern Mediterranean region (e.g. Finné et al. 2011).

Conclusions

- Pollen data from the north and SE Aegean basins and the northern Levantine Basin record an expansion of forest cover after ~5.4 ka BP that is attributed to an increase in available humidity. In addition, marine proxies clearly support ongoing warm and humid conditions between 5.5 and 4.0 ka BP and the establishment of relatively stratified conditions of the upper water column not only in the semi-enclosed Aegean basins but also in the deep northern Levantine Basin. During this interval, SST fluctuates in the Aegean Sea; however, it exhibits a clear positive shift at ~4.8 ka BP. This pattern allows us to conclude that certain climatic factors favoured fluvial discharge, amplified nutrient inputs and established relatively high productive conditions during the Mid-Holocene, leading to the deposition of a sapropel-like layer only in the SE Aegean site.
- The warm and humid climatic conditions triggered upper water column stratification and enhancement of the DCM, resulting in the establishment of dysoxic conditions in the shallow basins. In contrast to the shallow SE Aegean, the deeper North Aegean and the deepest northern Levantine sites, although experiencing stratification in the upper parts of the water column, did not develop bottom-water dysoxia. Thus, a top–down mechanism of stratification–DCM development–fast transport and burial of organic matter is the most reasonable explanation for the preservation of the productivity signal in shallow sites, leading to a sapropel-like expression during the warm and humid Mid-Holocene.
- Our evidence from the north and SE Aegean and the northern Levantine may reflect the continuing albeit weak Mid-Holocene South Asian monsoon forcing combined with lighter Etesian winds. The termination of the Mid-Holocene warm and humid phase coincides with the "4.2 ka" significant Northern Hemisphere rapid climate cooling. Our humidity evidence exhibits an N–S time transgressive aridification gradient in the Aegean Sea. The persistence of humid conditions in the southern parts of the Aegean Sea is most probably associated with the reorganization of the general atmospheric circulation, leading to a further southward migration of the ITCZ in the tropics during the Mid-Holocene.

Acknowledgments This work has been made possible thanks to the financial support provided by the EraNet/Marinera Medecos project and University of Athens/Kapodistrias research grant. The authors kindly acknowledge Mira Bar-Matthews for providing $\delta^{13}C$ data from the Soreq cave. Thoughtful discussions with Neil Roberts are greatly appreciated. Critical comments by Phil Meyers and an anonymous reviewer have proved essential in improving the manuscript.

References

Almogi-Labin A, Bar-Matthews M, Shriki D, Kolosovsky E, Paterne M, Schilman B, Ayalon A, Aizenshtat Z, Matthews A (2009) Climatic variability during the last ~90 ka of the southern and northern Levantine basin as evident from marine records and speleothems. Quat Sci Rev 28:2882–2896

Bar-Matthews M, Ayalon A (2011) Mid-Holocene climate variations revealed by high-resolution speleothem records from Soreq Cave, Israel and their correlation with cultural changes. Holocene 21:163–171

Bar-Matthews M, Ayalon A, Gilmour M, Hawkesworth CJ (2003) Sea-land oxygen isotopic relationships from planktonic foraminifera and speleothems in the Eastern Mediterranean region and their implication for paleorainfall during interglacial intervals. Geochim Cosmochim Acta 67:3181–3199

Beaufort L, De Garidel-Thoron T, Mix AC, Pisias NG (2001) ENSO-like forcing on oceanic primary production during the late Pleistocene. Science 293:2440–2444

Bethoux JP, Gentili B, Morin P, Nicolas E, Pierre C, Ruiz-Pino D (1999) The Mediterranean Sea: a miniature ocean for climatic and environmental studies and a key for the climatic functioning of the north Atlantic. Progr Oceanogr 44:131–146

Cacho I, Grimalt JO, Canals M (2002) Response of the western Mediterranean Sea to rapid climatic variability during the last 50,000 years: a molecular biomarker approach. J Mar Syst 33–34:253–272

Casford JSL, Rohling EJ, Abu-Zied RH, Fontanier C, Jorissen FJ, Leng MJ, Schmiedl G, Thomson J (2003) A dynamic concept for eastern Mediterranean circulation and oxygenation during sapropel formation. Palaeogeogr Palaeoclimatol Palaeoecol 190:103–119

Casford JSL, Abu-Zied R, Rohling EJ, Cooke S, Fontanier CH, Leng M, Millard A, Thomson J (2007) A stratigraphically controlled multi-proxy chronostratigraphy for the eastern Mediterranean. Paleoceanography 22:PA4215. doi:10.1029/2007PA001422

Castañeda IS, Schefuß E, Pätzold J, Damsté JS, Weldeab S, Schouten S (2010) Millennial-scale sea surface temperature changes in the Eastern Mediterranean (Nile River delta region) over the last 27,000 years. Paleoceanography 25:PA1208. doi:10.1029/2009PA001740

Castradori D (1993) Calcareous nannofossil and the origin of Eastern Mediterranean sapropels. Paleoceanography 8:459–471

Çatağay MN, Görür N, Algan O, Eastoe C, Tchapalyga A, Ongan D, Kuhn T, Kuşcu I (2000) Late Glacial–Holocene palaeoceanography of the Sea of Marmara: timing of connections with the Mediterranean and the Black Seas. Mar Geol 167:191–206

Crudeli D, Young JR, Erba E, Geisen M, Ziveri P, de Lange GJ, Slomp CP (2006) Fossil record of holococcoliths and selected hetero-holococcolith associations from the Mediterranean (Holocene–late Pleistocene): evaluation of carbonate diagenesis and paleoecological–paleogeographic implications. Palaeogeogr Palaeoclimatol Palaeoecol 237:191–212

Cullen HM, de Menocal PB, Hemming S, Hemming G, Brown FH, Guilderson T, Sirocko F (2000) Climate change and the collapse of the Akkadian empire: evidence from the deep sea. Geology 28:379–382

de Lange GJ, Ten Haven HL (1983) Recent sapropel formation in the eastern Mediterranean. Nature 305:797–798

de Lange GJ, Thomson J, Reitz A, Slomp CP, Principato MS, Erba E, Corselli C (2008) Synchronous basin-wide formation and redox-controlled preservation of a Mediterranean sapropel. Nat Geosci 1:606–610

de Menocal PB, Ortiz J, Guilderson T, Adkins J, Sarnthein M, Baker L, Yarusinsky M (2000) Abrupt onset and termination of the

African humid period: rapid climate responses to gradual insolation forcing. Quat Sci Rev 19:347–361

di Donato V, Esposito P, Russo-Ermolli E, Scarano A, Cheddadi R (2008) Coupled atmospheric and marine palaeoclimatic reconstruction for the last 35 ka in the Sele Plain–Gulf of Salerno area (southern Italy). Quat Int 190:146–157

Dimiza M, Triantaphyllou MV, Dermitzakis MD (2008) Seasonality and ecology of living coccolithophores in E. Mediterranean coastal environments (Andros Island, middle Aegean Sea). Micropaleontology 54:159–175

Ehrmann W, Schmiedl G, Hamann Y, Kuhnt T, Hemleben C, Siebel W (2007) Clay minerals in Late Glacial and Holocene sediments of the northern and southern Aegean Sea. Palaeogeogr Palaeoclimatol Palaeoecol 249:36–57

Emeis K-C, Struck U, Schulz H-M, Rosenberg R, Bernasconi S, Erlenkeuser H, Sakamoto T, Martinez-Ruiz F (2000) Temperature and salinity variations of Mediterranean Sea surface waters over the last 16,000 years from records of planktonic stable oxygen isotopes and alkenone unsaturation ratios. Palaeogeogr Palaeoclimatol Palaeoecol 158:259–280

Emeis K-C, Schulz H, Struck U, Rossignol-Strick M, Erlenkeuser H, Howell MW, Kroon D, Mackensen A, Ishizuka S, Oba T, Sakamoto T, Koizumi I (2003) Eastern Mediterranean surface water temperatures and $\delta^{18}O$ composition during deposition of sapropels in the late Quaternary. Paleoceanography 18:1005. doi:10.1029/2000PA0006117

Facorellis Y, Maniatis Y, Kromer B (1998) Apparent ^{14}C ages of marine mollusk shells from a Greek island: calculation of the marine reservoir effect in the Aegean Sea. Radiocarbon 40:963–973

Finné M, Holmgren K, Sundqvist HS, Weiberg E, Lindblom M (2011) Climate in the eastern Mediterranean, and adjacent regions, during the past 6000 years—a review. J Archaeol Sci 38:3153–3173

Flores JA, Barcena MA, Sierro FJ (2000) Ocean-surface and wind dynamics in the Atlantic Ocean off northwest Africa during the last 140,000 years. Palaeogeogr Palaeoclimatol Palaeoecol 161:459–478

Gaetani M, Baldi M, Dalu GA, Maracchi G (2007) Connessioni tra il clima della regione Mediterranea e l'Africa occidentale attraverso la circolazione meridiana di Hadley. In: Carli B, Cavarretta G, Colacino M, Fuzzi S (eds) Clima e cambiamenti climatici. Consiglio Nazionale delle Ricerche, Roma, pp 23–26

Gallego-Torres D, Martinez-Ruiz F, Meyers PA, Paytan A, Jimenez-Espejo FJ, Ortega-Huertas M (2011) Productivity patterns and N-fixation associated with Pliocene–Holocene sapropels: paleoceanographic and paleoecological significance. Biogeosciences 8:415–431

Gasse F (2000) Hydrological changes in the African tropics since the last glacial maximum. Quat Sci Rev 19:189–211

Gasse F, van Campo E (1994) Abrupt post-glacial climate events in west Asia and north Africa monsoon domains. Earth Planet Sci Lett 126:435–456

Geraga M, St Tsaila-Monopoli, Ioakim CH, Papatheodorou G, Ferentinos G (2000) An evaluation of paleoenvironmental changes during the last 18,000 yr BP in the Myrtoon Basin, SW Aegean Sea. Palaeogeogr Palaeoclimatol Palaeoecol 156:1–17

Geraga M, Ioakim C, Lykousis V, Tsaila-Monopolis S, Mylona G (2010) The high resolution palaeoclimatic and palaeoceanographic history of the last 24,000 years in the central Aegean Sea, Greece. Palaeogeogr Palaeoclimatol Palaeoecol 287:101–115

Giunta S, Negri A, Morigi C, Capotondi L, Combourieu-Nebout N, Emeis KC, Sangiorgi F, Vigliotti L (2003) Coccolithophorid ecostratigraphy and multi-proxy paleoceanographic reconstruction in the Southern Adriatic Sea during the last deglacial time (Core AD91-17). Palaeogeogr Palaeoclimatol Palaeoecol 190:39–59

Gogou A, Bouloubassi I, Lykousis V, Arnaboldi M, Gaitani P, Meyers PA (2007) Organic geochemical evidence of abrupt Late Glacial–Holocene climate changes in the North Aegean Sea. Palaeogeogr Palaeoclimatol Palaeoecol 256:1–20

Gupta AK, Anderson DM, Overpeck JT (2003) Abrupt changes in Asian southwest monsoon during the Holocene and their links to the North Atlantic Ocean. Nature 421:354–356

Gupta AK, Das M, Anderson DM (2005) Solar influence on the Indian summer monsoon during the Holocene. Geophys Res Lett 32:L17703. doi:10.1029/2005GL022685

Hilgen FJ, Abdul Aziz H, Krijgsman W, Raffi I, Turco E (2003) Integrated stratigraphy and astronomical tuning of the Serravallian and lower Tortonian at Monte dei Corvi (Middle–Upper Miocene, northern Italy). Palaeogeogr Palaeoclimatol Palaeoecol 199:229–264

Incarbona A, Bonomo S, Di Stefano E, Zgozi S, Essarbout N, Talha M, Tranchida G, Bonanno A, Patti B, Placenti F, Buscaino G, Cuttitta A, Basilone G, Bahri T, Massa F, Censi P, Mazzola S (2008) Calcareous nannofossil surface sediment assemblages from the Sicily Channel (central Mediterranean Sea), Palaeoceanographic implications. Mar Micropaleontol 67:297–309

Ioakim C, Triantaphyllou M, Tsaila-Monopolis S, Geraga M, Dimiza M, Lykousis V (2009) New micropalaeontological records of eastern Mediterranean marine sequences recovered offshore of Crete, during HERMES cruise and their palaeoclimatic-palaeoceanographic significance. Acta Nat "L'Ateneo Parmense" 45:152

Katsouras G, Gogou A, Bouloubassi I, Emeis K-C, Triantaphyllou M, Roussakis G, Lykousis V (2010) Organic carbon distribution and isotopic composition in three records from the eastern Mediterranean Sea during the Holocene. Org Geochem 41:935–939

Kotthoff U, Müller UC, Pross J, Schmiedl G, Lawson IT, Van De Schootbrugge B, Schulz H (2008a) Late glacial and Holocene vegetation dynamics in the Aegean region: an integrated view based on pollen data from marine and terrestrial archives. Holocene 18:1019–1032

Kotthoff U, Pross J, Müller UC, Peyron O, Schmiedl G, Schulz H, Bordon A (2008b) Climate dynamics in the borderlands of the Aegean Sea during formation of sapropel S1 deduced from a marine pollen record. Quat Sci Rev 27:832–845

Koukousioura O, Dimiza MD, Triantaphyllou MV, Hallock P (2011) Living benthic foraminifera as an environmental proxy in coastal ecosystems: a case study from the Aegean Sea (Greece, NE Mediterranean). J Mar Syst 88:489–501

Kouli K, Gogou A, Bouloubassi I, Triantaphyllou M, Ioakim C, Katsouras G, Roussakis G, Lykousis V (2012) Late postglacial paleoenvironmental change in the northeastern Mediterranean region, Combined palynological and molecular biomarker evidence. Quat Int 261:118–127

Kuhnt T, Schmiedl G, Ehrmann W, Hamann Y, Hemleben C (2007) Deep-sea ecosystem variability of the Aegean Sea during the past 22 kyr as revealed by Benthic Foraminifera. Mar Micropaleontol 64:141–162

Lario J, Sanchez-Moral S, Fernandez V, Jimeno A, Menendezlario M (1997) Palaeoenvironmental evolution of the Blue Nile (central Sudan) during the early and mid-Holocene (Mesolithic–Neolithic transition). Quat Sci Rev 16:583–588

Lespez L (2003) Geomorphic responses to long-term land use changes in Eastern Macedonia (Greece). Catena 51:181–208

Lie O, Dahl SO, Nesje A, Matthews JA, Sandvold S (2004) Holocene fluctuations of a polythermal glacier in high-alpine eastern Jotunheimen, central–southern Norway. Quat Sci Rev 2:1925–1945

Lionello P, Malanotte-Rizzoli P, Boscolo R, Alpert P, Artale V, Li L, Luterbacher J, May W, Trigo R, Simplis MT, Ulbrich U, Xoplaki E (2006) The Mediterranean climate: an overview of the main characteristics and issues. In: Lionello P, Malanotte-Rizzoli P, Boscolo R (eds) Mediterranean climate variability. Elsevier, Amsterdam, pp 1–26

Luterbacher J, Xoplaki E (2003) 500-year winter temperature and precipitation variability over the Mediterranean area and its connection to the large-scale atmospheric circulation. In: Bolle HJ (ed) Mediterranean climate. Variability and trends. Springer, Berlin, pp 133–153

Lykousis V, Chronis G (1989) Mechanisms of sediment transport and deposition: sediment sequences and accumulation during the Holocene on the Thermaikos plateau, the continental slope, and basin (Sporadhes basin), northwestern Aegean sea, Greece. Mar Geol 87:5–26

Lykousis V, Chronis G, Tselepides A, Price NB, Theocharis A, Siokou-Fragou I, Van Wambeke F, Danovaro R, Stavrakakis S, Duineveld G, Georgopoulos D, Ignatiades L, Souvermezoglou A, Voutsinou-Taliadouri F (2002) Major outputs of the recent multidisciplinary biogeochemical researches undertaken in the Aegean Sea. J Mar Syst 33–34:313–334

Magny M, Vannière B, Zanchetta G, Fouach E, Touchais G, Petrika L, Coussot C, Walter-Simonnet AV, Arnaud F (2009) Possible complexity of the climatic event around 4300–3800 cal BP in the central and western Mediterranean. Holocene 19:823–833

Magny M, Vannière B, Calo C, Millet L, Leroux A, Peyron O, Zanchetta G, La Mantia T, Tinner W (2011) Holocene hydrological changes in south-western Mediterranean as recorded by lake-level fluctuations at Lago Preola, a coastal lake in southern Sicily, Italy. Quat Sci Rev 30:2459–2475

Magny M, Peyron O, Sadori L, Ortu E, Zanchetta G, Vannière B, Tinner W (2012) Contrasting patterns of precipitation seasonality during the Holocene in the south- and north-central Mediterranean. J Quat Sci 27:290–296

Malanotte-Rizzoli P, Manca BB, Ribera d'Alcalà M, Theocharis A, Bergamasco A, Bregant D, Budillon G, Civitarese G, Georgopoulos D, Michelato A, Sansone E, Scarazzato P, Souvermezoglou E (1997) A synthesis of the Ionian Sea hydrography, circulation and water mass pathways during POEM-Phase I. Prog Oceanogr 39:153–204

Margari V, Gibbard PL, Bryant CL, Tzedakis PC (2009) Character of vegetational and environmental changes in southern Europe during the last glacial period; evidence from Lesvos Island, Greece. Quat Sci Rev 28:1317–1339

Marino G, Rohling EJ, Rijpstra WI, Sangiorgi F, Schouten S, Sinninghe Damsté JS (2007) Aegean Sea as driver of hydrological and ecological changes in the eastern Mediterranean. Geology 35:675–678

Marino G, Rohling EJ, Sangiorgi F, Hayes A, Casford JSL, Lotter AF, Kucera M, Brinkhuis H (2009) Early and middle Holocene in the Aegean Sea: interplay between high and low latitude climate variability. Quat Sci Rev 28:3246–3262

Mayewski PA, Rohling E, Stager CJ, Karlen W, Maasch KA, Meeker LD, Meyerson EA, Gasse F, van Kreveld S, Holmgren K, Lee-Thorp J, Rosqvist G, Rack F, Staubwasser M, Schneider RR, Steig E (2004) Holocene climate variability. Quat Res 62:243–255

Meier KJS, Zonneveld KAF, Kasten S, Willems H (2004) Different nutrient sources forcing increased productivity during eastern Mediterranean S1 sapropel formation as reflected by calcareous dinoflagellate cysts. Paleoceanography 19:1012. doi: 10.1029/2003PA000895

Migowski C, Mordechai S, Prasad S, Negendank JFW, Agnon A (2006) Holocene climate variability and cultural evolution in the Near East from the Dead Sea sedimentary record. Quat Res 66:421–431

Möbius J, Lahajnar N, Emeis K-C (2010) Diagenetic control of nitrogen isotope ratios in Holocene sapropels and recent sediments from the Eastern Mediterranean Sea. Biogeosciences 7:3901–3914

Molfino B, Mcintyre A (1990) Precessional forcing of nutricline dynamics in the equatorial Atlantic. Science 249:766–769

Moodley L, Middelburg JJ, Herman PMJ, Soetaert K, de Lange GJ (2005) Oxygenation and organic-matter preservation in marine sediments: direct experimental evidence from ancient organic carbon-rich deposits. Geology 33:889–892

Müller PJ, Kirst G, Ruhland G, von Storch L, Rosell-Mele A (1998) Calibration of the alkenone paleotemperature index $U^{k'}_{37}$ based on core tops from the eastern South Atlantic and the global ocean (60°N–60°S). Geochim Cosmochim 62:1757–1772

Okada H, Honjo S (1973) The distribution of ocean coccolithophorids in the Pacific. Deep-Sea Res 20:355–374

Pavlopoulos K, Karkanas P, Triantaphyllou M, Karymbalis E, Tsourou T, Palyvos N (2006) Paleoenvironmental evolution of the coastal plain of Marathon, Greece, during the Late Holocene: depositional environment, climate, and sea level changes. J Coast Res 22:424–438

Pavlopoulos K, Kapsimalis V, Theodorakopoulou K, Panagiotopoulos IP (2011) Vertical displacement trends in the Aegean coastal zone (NE Mediterranean) during the Holocene assessed by geo-archaeological data. Holocene 22:717–728

Perner K, Moros M, Jennings A, Lloyd JM, Knudsen KL (2012) Millenial to centennial scale climate cycling in Disco Bugt, West Greenland. In: Foraminifera and nanofossil groups joint meeting 2012. The Micropaleontological Society, Edinburgh. Book of Abstracts, p 37

Peyron O, Goring S, Dormoy I, Kotthoff U, Pross J, Beaulieu J-L, Drescher-Schneider R, Vannière B, Magny M (2011) Holocene seasonality changes in the central Mediterranean region reconstructed from the pollen sequences of Lake Accesa (Italy) and Tenaghi Philippon (Greece). Holocene 21:131–146

Piper DJ, Perissoratis C (1991) Late Quaternary sedimentation on the North Aegean continental margin, Greece. Bull Am Assoc Petrol Geol 75:46–61

Piva A, Asioli A, Trincardi F, Schneider RR, Vigliotti L (2008) Late-Holocene climate variability in the Adriatic Sea (central Mediterranean). Holocene 18:153–167

Poulos SE (2009) Origin and distribution of the terrigenous component of the unconsolidated surface sediment of the Aegean floor: a synthesis. Cont Shelf Res 2:2045–2060

Poulos SE, Drakopoulos PG, Collins MB (1997) Seasonal variability in sea surface oceanographic conditions in the Aegean Sea (Eastern Mediterranean), an overview. J Mar Syst 13:225–244

Poynter JG, Eglinton G (1990) Molecular composition of three sediments from hole 717C: the Bengal Fan. Proc Ocean Drill Prog Sci Res 116:155–161

Reimer PJ, McCormac FG (2002) Marine radiocarbon reservoir corrections for the Mediterranean and Aegean Seas. Radiocarbon 44:159–166

Roberts N, Brayshaw D, Kuzucuoğlu C, Perez R, Sadori L (2011a) The mid-Holocene climatic transition in the Mediterranean: causes and consequences. Holocene 21:3–12

Roberts N, Eastwood W, Kuzucuoğlu C, Fiorentino G, Carracuta V (2011b) Climate, vegetation and cultural change in the eastern Mediterranean during the mid-Holocene environmental transition. Holocene 21:147–162

Robinson SA, Black S, Sellwood BW, Valdes PJ (2006) A review of paleoclimates and paleoenvironments in the Levant and eastern Mediterranean from 25,000 to 5,000 years BP: setting the environmental background for the evolution of human civilisation. Quat Sci Rev 25:1517–1541

Rohling EJ, Cane TR, Cooke S, Sprovieri M, Bouloubassi I, Emeis KC, Schiebel R, Kroon D, Jorissen FJ, Lorre A, Kemp AES (2002a) African monsoon variability during the previous interglacial maximum. Earth Planet Sci Lett 202:61–75

Rohling EJ, Mayewski PA, Abu-Zied RH, Casford JSL, Hayes A (2002b) Holocene atmosphere–ocean interactions: records from Greenland and the Aegean Sea. Clim Dyn 18:587–593

Rohling EJ, Abu-Zied RH, Casford JSL, Hayes A, Hoogakker BAA (2009) The marine environment: present and past. In: Woodward JC (ed) The physical geography of the Mediterranean. Oxford University Press, Oxford, pp 33–67

Rossignol-Strick M, Nesteroff W, Olive P, Vergnaud-Grazzini C (1982) After the deluge: Mediterranean stagnation and sapropel formation. Nature 295:105–110

Roussakis G, Karageorgis AP, Conispoliatis N, Lykousis V (2004) Last glacial–Holocene sediment sequences in N. Aegean basins, structure, accumulation rates and clay mineral distribution. Geo-Mar Lett 24:97–111

Sadori L, Jahns S, Peyron O (2011) Mid-Holocene vegetation history of the central Mediterranean. Holocene 21:117–129

Schmiedl G, Kuhnt T, Ehrmann W, Emeis K-C, Hamann Y, Kotthoff U, Dulski P, Pross J (2010) Climatic forcing of eastern Mediterranean deep-water formation and benthic ecosystems during the past 22,000 years. Quat Sci Rev 29:3006–3020

Sperling M, Schmiedl G, Hemleben Ch, Emeis K-C, Erlenkeuser H, Grootes PM (2003) Black Sea impact on the formation of eastern Mediterranean sapropel S1? Evidence from the Marmara Sea. Palaeogr Palaeoclimatol Palaeoecol 190:9–21

Thamban M, Kawahata H, Purnachandra Rao V (2007) Indian summer monsoon variability during the holocene as recorded in sediments of the arabian sea: timing and implications. J Oceanogr 63:1009–1020

Theocharis A, Balopoulos E, Kioroglou S, Kontoyiannis H, Iona A (1999) A synthesis of the circulation and hydrography of the South Aegean and the Straits of Cretan Arc (March 1994–January 1995). Progr Oceanogr 44:469–509

Tolun L, Çağatay MN, Carrigan WJ (2002) Organic geochemistry and origin of Late Glacial–Holocene sapropelic layers and associated sediments in Marmara Sea. Mar Geol 190:47–60

Triantaphyllou MV, Antonarakou A, Kouli K, Dimiza M, Kontakiotis G, Papanikolaou M, Ziveri P, Mortyn PG, Lianou V, Lykousis V, Dermitzakis MD (2009a) Late Glacial–Holocene ecostratigraphy of the south-eastern Aegean Sea, based on plankton and pollen assemblages. Geo-Mar Lett 29:249–267

Triantaphyllou MV, Ziveri P, Gogou A, Marino G, Lykousis V, Bouloubassi I, Emeis K-C, Kouli K, Dimiza M, Rosell-Mele A, Papanikolaou M, Katsouras G, Nunez N (2009b) Late Glacial–Holocene climate variability at the south-eastern margin of the Aegean Sea. Mar Geol 266:182–197

Tyrlis E, Lelieveld J, Steil B (2012) The summer circulation in the eastern mediterranean and the middle east: influence of the south asian monsoon and mid-latitude dynamics. In: Helmis CG, Nastos PT (eds) Advances in Meteorology, Climatology and Atmospheric Physics. Springer Atmospheric Sciences, pp 793–802

Tzedakis PC, Frogley MR, Lawson IT, Preece RC, Cacho I, De Abreu L (2004) Ecological thresholds and patterns of millennial-scale climate variability: the response of vegetation in Greece during the last glacial period. Geology 32:109–112

Versteegh GJM, Zonneveld KAF, de Lange GJ (2010) Selective aerobic and anaerobic degradation of lipids and palynomorphs in the Eastern Mediterranean since the onset of sapropel S1 deposition. Mar Geol 278:177–192

Wang Y, Cheng H, Edwards RL, He Y, Kong X, An Z, Wu J, Kelly MJ, Dykoski CA, Li X (2005) The holocene asian monsoon: links to solar changes and north atlantic climate. Science 308:854–857

Wanner H, Beer J, Bütikofer J, Crowley TJ, Cubasch U, Flückiger J, Goosse H, Grosjean M, Joos F, Kaplan JO, Küttel M, Müller SA, Prentice IC, Solomina O, Stocker TF, Tarasov P, Wagner M, Widmannm M (2008) Mid- to Late Holocene climate change: an overview. Quat Sci Rev 27:1791–1828

Weiss H, Courty MA, Wetterstorm W, Guichard F, Senior L, Meadow R, Curnow A (1993) The genesis and collapse of third millennium north Mesopotamia civilization. Science 261:995–1004

Wick L, Lemcke G, Sturm M (2003) Evidence of Late glacial and Holocene climatic change and human impact in eastern Anatolia: high-resolution pollen, charcoal, isotopic and geochemical records from the laminated sediments of Lake Van, Turkey. Holocene 13:665–667

Young JR (1994) Functions of coccoliths. In: Winter A, Siesser WG (eds) Coccolithophores. Cambridge University Press, Cambridge, pp 13–27

Zervakis V, Georgopoulos D, Drakopoulos PG (2000) The role of the North Aegean in triggering the recent Eastern Mediterranean climatic changes. J Geophys Res 105:26103–26116

Zhou W, Zheng Y, Meyers PA, Jull AJT, Xie S (2010) Postglacial climate-change record in biomarker lipid compositions of the Hani peat sequence, northeastern China. Earth Planet Sci Lett 294:37–46

Zonneveld KAF, Bockelmann F, Holzwarth U (2007) Selective preservation of organic-walled dinoflagellate cysts as a tool to quantify past net primary production and bottom water oxygen concentrations. Mar Geol 237:109–126